CRYSTALLOGRAPHIC COMMUNICATIONS

ISSN 2056-9890

Synthesis, crystal structure and Hirshfeld surface analysis of a 1:1 salt of sparfloxacin and 4-aminosalicylic acid

Bhumi C. Patel,[a] Krunal M. Modi[b,c]* and J. Prakasha Reddy[d]*

[a]Department of Chemistry, School of Sciences, Indrashil University, Rajpur, 382740, India, [b]Department of Chemisry, School of Engineering, Indrashil University, Rajpur 382740, India, [c]Department of Chemistry, Faculty of Science, Gokul Global University,Sidhpur, Gujarat, 384151, India, and [d]Department of Applied Chemistry, School of Applied Material Sciences, Central University of Gujarat, Kundhela 391107, India. *Correspondence e-mail: krunal.modi@indrashiluniversity.ac.in, j.prakashareddy@cug.ac.in

Received 20 May 2026
Accepted 29 May 2026

Edited by L. Van Meervelt, Katholieke Universiteit Leuven, Belgium

Keywords: crystal structure; sparfloxacinium 4-aminosalicylate salt; Hirshfeld; X-ray diffraction; hydrogen-bonding interactions.

CCDC reference: 2558235

Supporting information: this article has supporting information at journals.iucr.org/e

The anhydrous salt of sparfloxacin [5-amino-1-cyclopropyl-7-(3,5-dimethylpiperazin-1-yl)-6,8-difluoro-4-oxo-1,4-dihydroquinoline-3-carboxylic acid] with 4-aminosalicylic acid, $C_{22}H_{22}F_2N_4O_3^{+}\cdot C_7H_6NO_3^{-}$, features both intermolecular (N—H···O) and intramolecular (O—H···O) interactions. In the crystal, two sparfloxacin and two 4-aminosalicylic acid molecules interact with each other through N—H···O hydrogen bonds, forming an $R_4^4(12)$ ring motif. The network of intermolecular interactions was further examined using Hirshfeld surface analysis and two-dimensional fingerprint plots.

1. Chemical context

Small molecules to peptides are well known for their esthetic appeal (Mehmood *et al.*, 2021; Patel *et al.*, 2021) and find various applications including in pharmaceutical chemistry (Shah *et al.*, 2023; Karmakar *et al.*, 2025; Gellman, 1998; Chauhan *et al.*, 2025). Fluoroquinones constitute broad spectrum antibiotics having many advantageous pharmacokinetic properties such as good oral bioavailability and large volume of distribution and are effective against Gram-positive and Gram-negative bacteria (Marona *et al.*, 2001; Jain *et al.*, 2002; Faria *et al.*, 2006). Apart from their use to cure infections in humans, they are also used in veterinary medicine as well as animal husbandry (poultry). A critical review of fluoroquinones with a focus on respiratory infections was reported (Zhanel *et al.*, 2002). Sparfloxacin, systematic name: 5-amino-1-cyclopropyl-7-(3,5-dimethylpiperazin-1-yl)-6,8-difluoro-4-oxo-1,4-dihydroquinoline-3-carboxylic acid, $C_{19}H_{22}F_2N_4O_3$, is a third-generation fluoroquinolone antibiotic, which is one of the most important and successful classes of man-made antibacterials with activity against a broad range of bacterial infections especially those affecting the acute exacerbations of chronic bronchitis, urinary tracts, soft tissue infections. bacterial conjunctivitis, *etc*., and prevents bacterial growth primarily by inhibiting the action of DNA gyrase. Reviews of sparfloxacin (Schentag, 2000), its antibacterial activity, pharmacokinetic properties, clinical efficacy, and tolerability in lower respiratory tract infections (Goa *et al.*, 1997), as well as a review on its penetration into the lower respiratory tract and sinuses have been published (Wise & Honeybourne, 1996). The electrostatic properties of nine fluoroquinolone antibiotics derived directly from their crystal-structure refinements was outlined (Holstein *et al.*, 2012). Photocatalytic degradation of sparfloxacin using nanoparticles of Ag–TiO_2

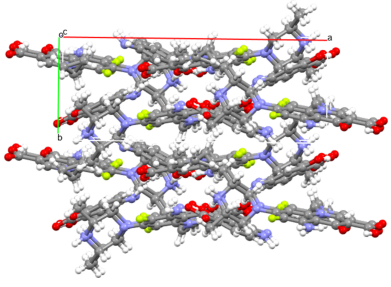

was reported (Kulkarni *et al.*, 2018). A new validated UV spectrophotometric method for the determination of sparfloxacin in tablets has been described (Sowjanya *et al.*, 2020). Details of sparfloxacin with inorganic ions $CuBr_4^{-}$ (Vasil'ev & Golovnev, 2014), $ZnBr_4^{2-}$ and $CdBr_4^{2-}$ (Vasil'ev & Golovnev, 2015) and BF_4^{-} (Shingnapurkar *et al.*, 2007) have also been published. Cocrystals of sparfloxacin with methyl, ethyl, propyl, and isobutyl *para*-hydroxybenzoic acids have been reported (Gunnam *et al.*, 2016). A sparfloxacin salt with pyrocatechuic acid (Zhang *et al.*, 2022) as well as salts with 2-(carboxymethyl)-2-hydroxybutanedioate, pyridine-3-carboxylate, 3-carboxybenzoate, 3-carboxyprop-2-enoate, and 2-aminobenzoate anions have been reported (Djaló *et al.*, 2021). Recently, three salts of sparfloxacin with one of the salts showing extended tapes of fused pentagonal water assemblies observed were reported (Shankara Prasad *et al.*, 2022). Continuing our research in the area of cocrystal chemistry (PrakashaReddy & Pedireddi, 2004), we have synthesized the title compound, which might be a potential solid dosage form if increases in solubility and/or dissolution enhancement are observed.

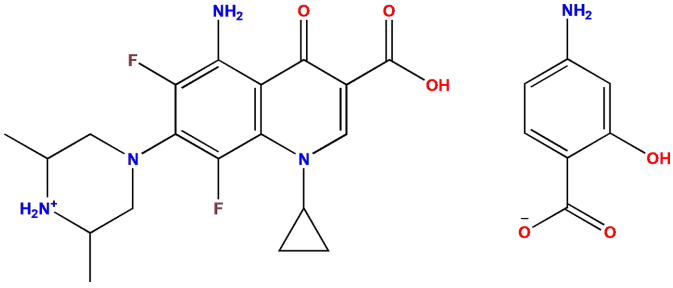

2. Structural commentary

Reaction between sparfloxacin and 4-aminosalicylic acid yielded the title salt, which crystallizes in the monoclinic $P2_1/n$ space group with one of each ion in the asymmetric unit. The crystals are solvent free and the molecular structure of the salt along with the atom labelling is shown in Fig. 1. Structurally, the sparfloxacinium cation is similar to those reported in the literature for other sparfloxacin structures and no unusual bond lengths or angles are observed. The quinoline ring along with the attached carboxyl, amino and fluorine atoms in the sparfloxacinium ion are essentially planar, with an r.m.s. deviation of 0.0631 Å and a largest deviation of 0.1621 (6) Å for atom F1. The dimethyl piperazine ring is oriented away from the quinoline ring, as illustrated by the C18—C19—N4—C24 torsion angle of 54.3 (3)° and the dihedral angle between the best planes through the quinoline ring system and the piperazine ring of 45.61 (9)°. For the cyclopropyl substituent, the C13—C11—N2—C14 torsion angle is 81.1 (3)° and the dihedral angle between the best planes through the quinoline ring system and the cyclopropyl ring is 54.2 (2)°.

The formation of a total of four intramolecular hydrogen bonds (Table 1; O1—H1···O2, O5—H5···O6, N3—H3*B*···F1 and N3—H3*A*···O6) is observed, formed between the hydroxy O atom of the –COOH group, the quinoline oxygen atom and the amino group present in sparfloxacin and the hydroxy group and adjacent oxygen atom present in the 4-aminosalicylic acid, resulting in *S*(5) and *S*(6) ring motifs (Fig. 1). This formation of intramolecular ring motifs is preserved, as can also be seen in other salts/co-crystals of sparfloxacin reported in the literature.

Table 1
Hydrogen-bond geometry (Å, °).

*Cg*6 is the centroid of the C2–C7 ring.

D—H···*A*	*D*—H	H···*A*	*D*···*A*	*D*—H···*A*
O1—H1···O2	1.02 (4)	1.60 (4)	2.529 (3)	149 (3)
N3—H3*A*···O6	0.86	1.92	2.648 (3)	142
N3—H3*A*···O1^{i}	0.86	2.52	2.965 (3)	113
N3—H3*B*···F1	0.91 (3)	2.29 (3)	2.637 (3)	102 (2)
O5—H5···O6	0.82	1.73	2.497 (3)	154
N5—H5*A*···O2^{ii}	0.99 (3)	1.74 (3)	2.715 (3)	167 (2)
N5—H5*B*···O3	0.91 (3)	1.85 (3)	2.754 (3)	172 (3)
N1—H1*B*···*Cg*6^{iii}	0.95 (4)	2.46 (5)	3.326 (3)	153 (4)

Symmetry codes: (i) $x+\frac{1}{2}, -y-\frac{1}{2}, z-\frac{1}{2}$; (ii) $-x, -y, -z+1$; (iii) $-x+\frac{1}{2}, y-\frac{1}{2}, -z+\frac{3}{2}$.

3. Supramolecular features

In the crystal structure, a dense network of strong intra- and intermolecular hydrogen bonding is observed. Crystal-structure analysis revealed that the cation–anion pair recognise through an N—H···O hydrogen-bonded $R_4^4(12)$ ring motif (Fig. 2, Table 1) with their inversion-related counterparts formed between piperazine the NH_2 group of the cation and the carboxylate group of the anion. These $R_4^4(12)$ ring motifs are further connected through C—H···O hydrogen bonding (Desiraju & Steiner, 1999; Patel *et al.*, 2024; Ramesh *et al.*, 2011). The crystal structure is further consolidated by N—H···π (Table 1) and C═O···π [C16═O16···*Cg*2; O16···*Cg*2 = 3.523 (2) Å; *Cg*2 is the centroid of the pyridine

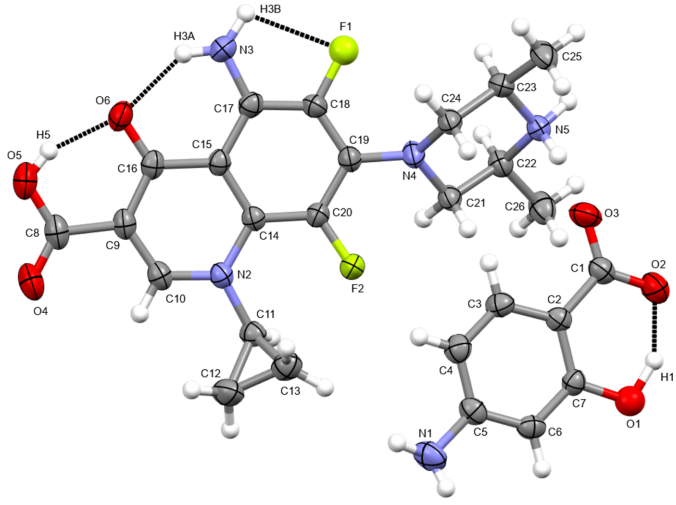

Figure 1
The molecular structure of the sparfloxacinium:4-aminosalicylate salt, showing the atom labelling and displacement ellipsoids drawn at the 30% probability level.

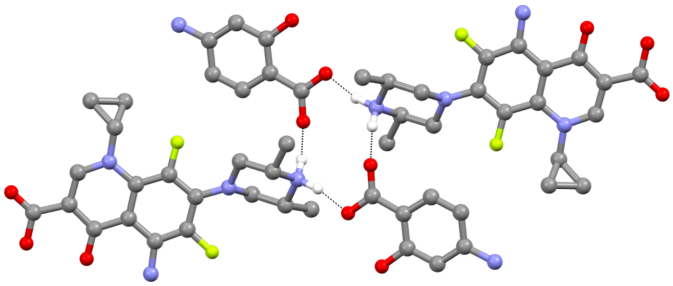

Figure 2
Recognition between the sparfloxacinium:4-aminosalicylate salt through N—H$^{+}\cdots$O^{-} interactions in the crystal.

ring N2/C9/C10/C14–C16] interactions. In addition, some π–π interactions are present in the crystal packing, *e.g.* between pyridine rings with a centroid-to-centroid distance of 3.6378 (12) Å. A three-dimensional projection along the crystallographic *c*-axis direction is shown in Fig. 3.

4. Hirshfeld surfaces and two-dimensional fingerprint plots

A Hirshfeld surface analysis and the corresponding fingerprint plots were generated using *CrystalExplorer* software (Spackman *et al.*, 2021; Spackman & Jayatilaka, 2009) to further investigate and quantify the contributions of the various intermolecular interactions in the crystal. The Hirshfeld surface mapped over $d_{\rm norm}$ and corresponding colours representing various interactions are shown in Fig. 4. The two-dimensional fingerprint plots (McKinnon *et al.*, 2007) for all intermolecular interactions and those delineated into specific contacts are shown in Fig. 5. The largest contribution comes from H$\cdots$H contacts at 46.3% of the total, which is consistent with the significant hydrogen content of the molecule. The next most important contact is O$\cdots$H/H$\cdots$O at 25.7%, which primarily comes from the intramolecular O—H$\cdots$O and

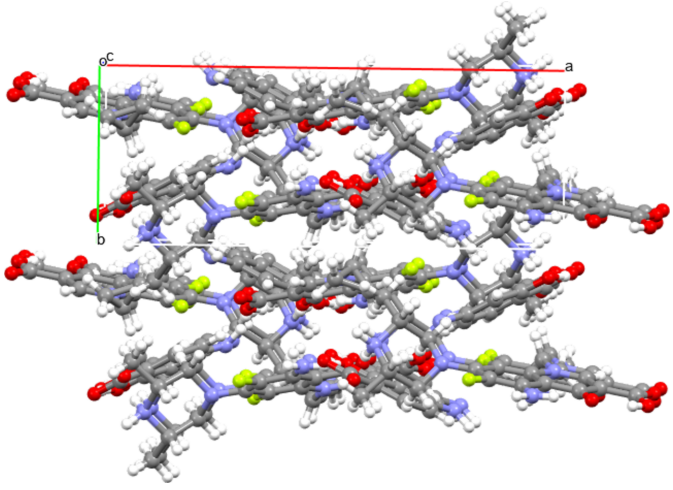

Figure 3
Three-dimensional packing viewed along the *c*-axis direction.

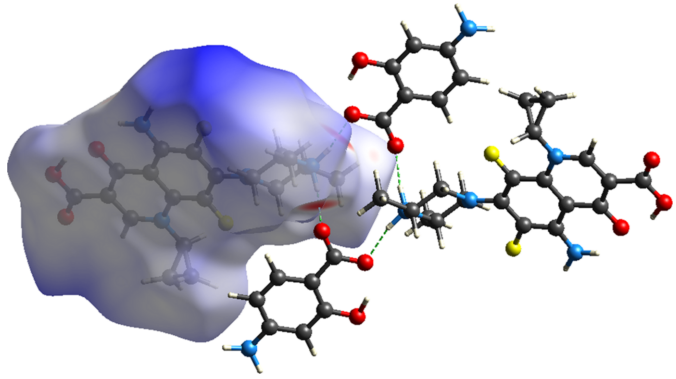

Figure 4
Hirshfeld surface mapped over $d_{\rm norm}$ showing N—H$^{+}\cdots$O^{-} intermolecular contacts.

intermolecular N—H$\cdots$O as well as C—H$\cdots$O interactions. The C$\cdots$H/H$\cdots$C interactions account for 7.1% while C$\cdots$C contacts contribute 6.7%, followed by F$\cdots$H/H$\cdots$F contacts contributing 5.4%. Further, 2.8 and 2.7% contributions corresponding to F$\cdots$O/O$\cdots$F and C$\cdots$O/O$\cdots$C contacts, respectively, are also observed.

5. Synthesis and crystallization

Sparfloxacin and 4-aminosalicylic acid were obtained from Aldrich, and HPLC-grade methanol was used for reaction. Sparfloxacin (100 mg, 0.255 mmol) was dissolved in methanol (10 ml) under constant stirring at 330 K for 30 min. An equimolar solution of 4-aminosalicylic acid (39 mg, 0.255 mmol) in methanol (10 ml) was added to the solution of sparfloxacin and stirring was continued further for about 30 min at 330 K. The mixture was cooled to room temperature and the solution was filtered. X-ray quality single crystals of suitable dimension were obtained over a period of five days by slow evaporation of the solvent.

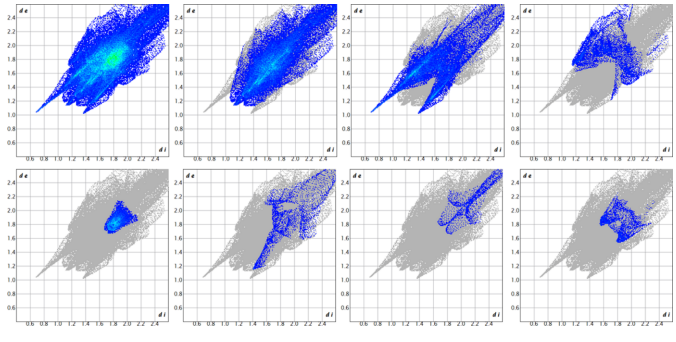

Figure 5
The full two-dimensional fingerprint plot for the title salt and those delineated into H$\cdots$H (46.3%), O$\cdots$H/H$\cdots$O (25.7%), C$\cdots$H/H$\cdots$C (7.1%), C$\cdots$C (6.7%), F$\cdots$H/H$\cdots$F (5.4%), F$\cdots$O/O$\cdots$F (2.8%) and C$\cdots$O/O$\cdots$C (2.7%) contacts.

6. Refinement

Crystal data, data collection and structure refinement details are summarized in Table 2. All hydrogen atoms were placed at idealized positions and refined using a riding model.

Acknowledgements

The authors are grateful to the Indrashil University and Central University of Gujarat, India, for research facilities. One of the authors (BCP) is indebted to the Knowledge Consortium of Gujarat (KCG), Department of Education, Government of Gujarat, India for a SHODH-Scheme fellowship.

Table 2
Experimental details.

Crystal data	
Chemical formula	$C_{19}H_{23}F_2N_4O_3^+\cdot C_7H_6NO_3^-$
M_r	545.54
Crystal system, space group	Monoclinic, $P2_1/n$
Temperature (K)	296
a, b, c (Å)	18.7603 (3), 7.15744 (10), 20.8511 (3)
β (°)	94.3739 (14)
V (Å^3)	2791.65 (7)
Z	4
Radiation type	Cu $K\alpha$
μ (mm^{-1})	0.87
Crystal size (mm)	0.29 × 0.21 × 0.12
Data collection	
Diffractometer	XtaLAB Synergy, Dualflex, HyPix
Absorption correction	Multi-scan (*CrysAlis PRO*; Rigaku OD, 2024)
T_{min}, T_{max}	0.416, 1.000
No. of measured, independent and observed [$I > 2\sigma(I)$] reflections	26903, 5468, 4535
R_{int}	0.030
(sin $\theta/\lambda)_{max}$ (Å^{-1})	0.624
Refinement	
$R[F^2 > 2\sigma(F^2)]$, $wR(F^2)$, S	0.064, 0.199, 1.08
No. of reflections	5468
No. of parameters	368
H-atom treatment	H atoms treated by a mixture of independent and constrained refinement
$\Delta\rho_{max}$, $\Delta\rho_{min}$ (e Å^{-3})	0.86, −0.72

Computer programs: *CrysAlis PRO* (Rigaku OD, 2024), *OLEX2.solve* (Bourhis *et al.*, 2015), *SHELXL2019/3* (Sheldrick, 2015) and *OLEX2* (Dolomanov *et al.*, 2009).

References

Bourhis, L. J., Dolomanov, O. V., Gildea, R. J., Howard, J. A. K. & Puschmann, H. (2015). *Acta Cryst.* A**71**, 59–75.

Chauhan, P., Maitra, R., Sangwan, S., Shah, S. K. H., Chopra, S., Reddy, J. P., Nangia, A. K. & Prabhakaran, P. (2025). *Chem. Asian J.* **20**, e70356.

Desiraju, G. R. & Steiner, T. (1999). *The Weak Hydrogen Bond in Structural Chemistry and Biology*. New York: Oxford University Press Inc.

Djaló, M., Cunha, A. E. S., Luís, J. P., Quaresma, S., Fernandes, A., André, V. & Duarte, M. T. (2021). *Cryst. Growth Des.* **21**, 995–1005.

Dolomanov, O. V., Bourhis, L. J., Gildea, R. J., Howard, J. A. K. & Puschmann, H. (2009). *J. Appl. Cryst.* **42**, 339–341.

Faria, A. F., de Souza, M. V. N., de Almeida, M. V. & de Oliveira, M. A. L. (2006). *Anal. Chim. Acta* **579**, 185–192.

Gellman, S. H. (1998). *Acc. Chem. Res.* **31**, 173–180.

Goa, K. L., Bryson, H. M. & Markham, A. (1997). *Drugs* **53**, 700–725.

Gunnam, A., Suresh, K., Ganduri, R. & Nangia, A. (2016). *Chem. Commun.* **52**, 12610–12613.

Holstein, J. J., Hübschle, C. B. & Dittrich, B. (2012). *CrystEngComm* **14**, 2520–2531.

Jain, S., Jain, N. K. & Pitre, K. S. J. (2002). *J. Pharm. Biomed. Anal.* **29**, 795–801.

Karmakar, S., Mallik, M., Sulava, S., Modi, U., Allu, S., Sangwan, S., Tothadi, S., Prakasha Reddy, J., Vasita, R., Nangia, A. K., Alone, D. P. & Prabhakaran, P. (2025). *Biomater. Sci.* **13**, 3828–3839.

Kulkarni, R. M., Malladi, R. S. & Hanagadakar, M. S. (2018). *Adv. Mat. Proc.* **3**, 526–529.

Marona, H. R. N. & Schapoval, E. E. S. (2001). *J. Pharm. Biomed. Anal.* **26**, 501–504.

McKinnon, J. J., Jayatilaka, D. & Spackman, M. A. (2007). *Chem. Commun*. pp. 3814–3816.

Mehmood, T. & Reddy, J. P. (2021). In *Progress in Molecular Biology and Translational Science* vol. 185, edited by R. S. Bhosale & V. Singh, pp. 179–198. New York: Academic Press.

Patel, K., Karmakar, S., Tothadi, S., Reddy, J. P. & Prabhakaran, P. (2024). *Chem. A Eur. J.* **30**, e202303757.

Patel, K., Shah, S. K. H. & Prabhakaran, P. (2021). In *Progress in Molecular Biology and Translational Science* vol. 185, edited by R. S. Bhosale & V. Singh, pp. 113–136. New York: Academic Press.

PrakashaReddy, J. & Pedireddi, V. R. (2004). *Tetrahedron* **60**, 8817–8827.

Ramesh, V. V. E., Roy, A., Vijayadas, K. N., Kendhale, A. M., Prabhakaran, P., Gonnade, R., Puranik, V. G. & Sanjayan, G. J. (2011). *Org. Biomol. Chem.* **9**, 367–369.

Rigaku OD (2024). *CrysAlis PRO*. Rigaku Corporation, Yarnton, England.

Schentag, J. J. (2000). *Clin. Ther.* **22**, 372–387.

Shah, S. K. H., Modi, U., Patel, K., James, A., N, S., De, S., Vasita, R. & Prabhakaran, P. (2023). *Biomater. Sci.* **11**, 6210–6222.

Shankara Prasad, H. J., Devaraju, Vinaya, Basavaraju, Y. B., Yathirajan, H. S. & Parkin, S. (2022). *Acta Cryst.* E**78**, 1257–1264.

Sheldrick, G. M. (2015). *Acta Cryst.* C**71**, 3–8.

Shingnapurkar, D., Butcher, R., Afrasiabi, Z., Sinn, E., Ahmed, F., Sarkar, F. & Padhye, S. (2007). *Inorg. Chem. Commun.* **10**, 459–462.

Sowjanya, M., Sirisha, C. & Prasad, M. K. (2020). *Rese. J. Pharm. Technol.* **13**, 3587–3592.

Spackman, M. A. & Jayatilaka, D. (2009). *CrystEngComm* **11**, 19–32.

Spackman, P. R., Turner, M. J., McKinnon, J. J., Wolff, S. K., Grimwood, D. J., Jayatilaka, D. & Spackman, M. A. (2021). *J. Appl. Cryst.* **54**, 1006–1011.

Vasil'ev, A. D. & Golovnev, N. N. (2014). *Russ. J. Inorg. Chem.* **59**, 322–325.

Vasiliev, A. D. & Golovnev, N. N. (2015). *J. Struct. Chem.* **56**, 907–911.

Wise, R. & Honeybourne, D. (1996). *J. Antimicrob. Chemother.* **37** Suppl. A, 57–63.

Zhanel, G. G., Ennis, K., Vercaigne, L., Walkty, A., Gin, A. S., Embil, J., Smith, H. & Hoban, D. J. (2002). *Drugs* **62**, 13–59.

Zhang, Y., Zhang, Y., Liu, L., Feng, Y., Wu, L., Zhang, L., Zhang, Y., Zou, D. & Liu, Y. (2022). *J. Mol. Struct.* **1250**, 131894.

supporting information

Acta Cryst. (2026). E**82** [https://doi.org/10.1107/S2056989026005736]

Synthesis, crystal structure and Hirshfeld surface analysis of a 1:1 salt of sparfloxacin and 4-aminosalicylic acid

Bhumi C. Patel, Krunal M. Modi and J. Prakasha Reddy

Computing details

4-[5-Amino-3-carboxy-1-cyclopropyl-6,8-difluoro-4-oxo-1,4-dihydroquinolin-7-yl]-2,6-dimethylpiperazin-1-ium 4-amino-2-hydroxybenzoate

Crystal data

$C_{19}H_{23}F_2N_4O_3^+ \cdot C_7H_6NO_3^-$
M_r = 545.54
Monoclinic, $P2_1/n$
a = 18.7603 (3) Å
b = 7.15744 (10) Å
c = 20.8511 (3) Å
β = 94.3739 (14)°
V = 2791.65 (7) Å^3
Z = 4
$F(000)$ = 1144
D_x = 1.298 Mg m^{-3}
Cu $K\alpha$ radiation, λ = 1.54184 Å
Cell parameters from 15825 reflections
θ = 3.0–74.2°
μ = 0.87 mm^{-1}
T = 296 K
Block, colourless
0.29 × 0.21 × 0.12 mm

Data collection

XtaLAB Synergy, Dualflex, HyPix diffractometer
Detector resolution: 10.0000 pixels mm^{-1}
ω scans
Absorption correction: multi-scan (CrysAlisPro; Rigaku OD, 2024)
T_{min} = 0.416, T_{max} = 1.000
26903 measured reflections
5468 independent reflections
4535 reflections with $I > 2\sigma(I)$
R_{int} = 0.030
θ_{max} = 74.3°, θ_{min} = 3.1°
h = −22→23
k = −6→8
l = −26→25

Refinement

Refinement on F^2
Least-squares matrix: full
$R[F^2 > 2\sigma(F^2)]$ = 0.064
$wR(F^2)$ = 0.199
S = 1.08
5468 reflections
368 parameters
0 restraints
Hydrogen site location: mixed
H atoms treated by a mixture of independent and constrained refinement
$w = 1/[\sigma^2(F_o^2) + (0.1004P)^2 + 1.2039P]$ where $P = (F_o^2 + 2F_c^2)/3$
$(\Delta/\sigma)_{max}$ = 0.001
$\Delta\rho_{max}$ = 0.86 e Å^{-3}
$\Delta\rho_{min}$ = −0.72 e Å^{-3}
Extinction correction: SHELXL2019/2 (Sheldrick 2015), $Fc^*=kFc[1+0.001xFc^2\lambda^3/\sin(2\theta)]^{-1/4}$
Extinction coefficient: 0.00063 (19)

Special details

Geometry. All esds (except the esd in the dihedral angle between two l.s. planes) are estimated using the full covariance matrix. The cell esds are taken into account individually in the estimation of esds in distances, angles and torsion angles; correlations between esds in cell parameters are only used when they are defined by crystal symmetry. An approximate (isotropic) treatment of cell esds is used for estimating esds involving l.s. planes.

Fractional atomic coordinates and isotropic or equivalent isotropic displacement parameters (Å²)

	x	*y*	*z*	U_{iso}*/U_{eq}
F2	0.33141 (7)	−0.1307 (3)	0.58770 (6)	0.0743 (4)
O6	0.56631 (9)	−0.3390 (3)	0.42044 (9)	0.0680 (5)
N2	0.48134 (9)	−0.1866 (3)	0.58847 (9)	0.0507 (4)
O5	0.68550 (9)	−0.3691 (3)	0.48149 (11)	0.0796 (6)
H5	0.653515	−0.370703	0.452402	0.119*
O2	−0.01246 (11)	−0.1420 (3)	0.63440 (10)	0.0835 (6)
N5	0.09720 (10)	−0.0477 (3)	0.45468 (10)	0.0546 (4)
H5A	0.0611 (14)	0.020 (4)	0.4266 (13)	0.066*
H5B	0.0779 (14)	−0.110 (4)	0.4874 (14)	0.066*
C20	0.36168 (11)	−0.1669 (3)	0.53233 (10)	0.0513 (5)
C14	0.43458 (11)	−0.1997 (3)	0.53226 (10)	0.0465 (5)
O3	0.05206 (11)	−0.2463 (3)	0.55722 (9)	0.0800 (6)
O4	0.69731 (10)	−0.3034 (3)	0.58457 (12)	0.0906 (7)
N4	0.24237 (9)	−0.1468 (3)	0.47622 (10)	0.0592 (5)
C17	0.41696 (12)	−0.2660 (3)	0.41633 (11)	0.0537 (5)
C24	0.19089 (12)	−0.2854 (3)	0.45037 (12)	0.0563 (5)
H24A	0.173551	−0.357309	0.485410	0.068*
H24B	0.214234	−0.370730	0.422507	0.068*
C16	0.53884 (12)	−0.2912 (3)	0.47192 (12)	0.0533 (5)
N3	0.43841 (13)	−0.3174 (4)	0.35779 (11)	0.0724 (6)
H3A	0.484477	−0.321564	0.359819	0.087*
C19	0.31507 (11)	−0.1793 (3)	0.47702 (11)	0.0514 (5)
C2	0.09910 (12)	−0.2787 (3)	0.66502 (10)	0.0512 (5)
C9	0.58140 (11)	−0.2758 (3)	0.53079 (12)	0.0555 (5)
C18	0.34517 (12)	−0.2265 (3)	0.42088 (10)	0.0544 (5)
C10	0.55099 (12)	−0.2224 (3)	0.58527 (12)	0.0556 (5)
H10	0.580734	−0.210068	0.622802	0.067*
C21	0.21160 (11)	−0.0136 (3)	0.51888 (11)	0.0545 (5)
H21A	0.247947	0.074656	0.534928	0.065*
H21B	0.194252	−0.078839	0.555368	0.065*
C15	0.46329 (11)	−0.2517 (3)	0.47310 (10)	0.0487 (5)
C7	0.09308 (12)	−0.2443 (3)	0.73051 (11)	0.0519 (5)
C11	0.45681 (12)	−0.1226 (3)	0.64947 (11)	0.0562 (5)
H11	0.439981	0.006979	0.649617	0.067*
C5	0.20952 (13)	−0.3765 (3)	0.75775 (12)	0.0588 (6)
C3	0.16136 (13)	−0.3667 (3)	0.64840 (11)	0.0592 (6)
H3	0.166266	−0.393645	0.605331	0.071*
C6	0.14795 (13)	−0.2905 (3)	0.77576 (11)	0.0574 (5)
H6	0.143489	−0.263401	0.818898	0.069*

N1	0.26501 (17)	−0.4184 (4)	0.80268 (15)	0.0834 (8)
C8	0.65916 (13)	−0.3161 (4)	0.53528 (16)	0.0687 (7)
C23	0.12860 (12)	−0.1927 (4)	0.41281 (11)	0.0579 (5)
H23	0.146013	−0.130730	0.375111	0.069*
C4	0.21548 (14)	−0.4149 (3)	0.69294 (12)	0.0636 (6)
H4	0.256253	−0.473365	0.679945	0.076*
C1	0.04328 (13)	−0.2201 (4)	0.61521 (12)	0.0608 (6)
C22	0.15077 (12)	0.0897 (3)	0.48317 (11)	0.0567 (5)
H22	0.169622	0.162133	0.448340	0.068*
C26	0.11441 (15)	0.2223 (4)	0.52730 (15)	0.0770 (8)
H26A	0.074505	0.281075	0.503798	0.116*
H26B	0.147855	0.316011	0.543166	0.116*
H26C	0.097888	0.153527	0.562811	0.116*
C25	0.07087 (15)	−0.3306 (5)	0.39044 (15)	0.0793 (8)
H25A	0.053401	−0.391960	0.427059	0.119*
H25B	0.090274	−0.421790	0.362854	0.119*
H25C	0.032303	−0.265493	0.367218	0.119*
C12	0.49327 (18)	−0.1882 (5)	0.71117 (14)	0.0880 (9)
H12A	0.531824	−0.277755	0.709146	0.106*
H12B	0.499333	−0.099296	0.746292	0.106*
C13	0.41968 (16)	−0.2517 (4)	0.69119 (13)	0.0728 (7)
H13A	0.413371	−0.380169	0.677069	0.087*
H13B	0.380889	−0.201766	0.714203	0.087*
F1	0.30262 (8)	−0.2317 (2)	0.36541 (7)	0.0718 (4)*
O1	0.03417 (11)	−0.1655 (3)	0.75118 (10)	0.0753 (5)*
H1	0.000 (2)	−0.157 (6)	0.7110 (19)	0.113*
H3B	0.4064 (16)	−0.320 (4)	0.3226 (15)	0.081 (9)*
H1A	0.252 (2)	−0.421 (6)	0.8376 (18)	0.102 (14)*
H1B	0.298 (2)	−0.509 (7)	0.790 (2)	0.123 (14)*

Atomic displacement parameters (Å²)

	U^{11}	U^{22}	U^{33}	U^{12}	U^{13}	U^{23}
F2	0.0503 (7)	0.1215 (13)	0.0515 (7)	0.0121 (8)	0.0064 (6)	−0.0052 (8)
O6	0.0546 (9)	0.0785 (11)	0.0734 (11)	0.0087 (8)	0.0207 (8)	0.0036 (9)
N2	0.0463 (9)	0.0521 (9)	0.0529 (10)	0.0015 (7)	−0.0011 (7)	0.0038 (8)
O5	0.0489 (9)	0.0809 (12)	0.1107 (15)	0.0062 (9)	0.0169 (10)	0.0025 (12)
O2	0.0698 (12)	0.0990 (14)	0.0793 (12)	0.0197 (11)	−0.0107 (10)	0.0046 (11)
N5	0.0446 (9)	0.0653 (11)	0.0531 (10)	0.0042 (8)	−0.0021 (8)	−0.0006 (9)
C20	0.0456 (11)	0.0588 (12)	0.0501 (11)	0.0018 (9)	0.0081 (9)	0.0010 (9)
C14	0.0442 (10)	0.0448 (10)	0.0503 (11)	−0.0007 (8)	0.0020 (8)	0.0060 (8)
O3	0.0837 (13)	0.1012 (15)	0.0528 (10)	−0.0111 (11)	−0.0094 (9)	0.0077 (9)
O4	0.0486 (10)	0.1061 (16)	0.1147 (17)	0.0052 (10)	−0.0091 (11)	0.0005 (13)
N4	0.0409 (9)	0.0695 (12)	0.0668 (12)	0.0016 (8)	0.0005 (8)	−0.0154 (9)
C17	0.0549 (12)	0.0547 (12)	0.0524 (12)	−0.0011 (9)	0.0096 (10)	0.0057 (9)
C24	0.0461 (11)	0.0635 (13)	0.0587 (12)	0.0001 (10)	0.0010 (9)	−0.0075 (10)
C16	0.0478 (11)	0.0462 (10)	0.0670 (13)	0.0010 (9)	0.0107 (10)	0.0088 (9)
N3	0.0593 (12)	0.1066 (18)	0.0525 (11)	0.0027 (12)	0.0129 (10)	−0.0044 (11)

C19	0.0431 (10)	0.0543 (11)	0.0565 (12)	0.0005 (9)	0.0027 (9)	0.0039 (9)
C2	0.0538 (12)	0.0488 (11)	0.0504 (11)	−0.0043 (9)	0.0006 (9)	0.0044 (9)
C9	0.0419 (11)	0.0501 (11)	0.0745 (15)	0.0003 (9)	0.0044 (10)	0.0086 (10)
C18	0.0508 (12)	0.0657 (13)	0.0459 (11)	−0.0004 (10)	−0.0021 (9)	0.0038 (9)
C10	0.0470 (11)	0.0520 (11)	0.0666 (14)	−0.0004 (9)	−0.0034 (10)	0.0062 (10)
C21	0.0432 (10)	0.0605 (12)	0.0590 (12)	−0.0011 (9)	−0.0012 (9)	−0.0072 (10)
C15	0.0448 (10)	0.0471 (10)	0.0548 (12)	0.0000 (8)	0.0077 (9)	0.0066 (9)
C7	0.0501 (11)	0.0528 (11)	0.0538 (12)	0.0000 (9)	0.0098 (9)	0.0036 (9)
C11	0.0584 (12)	0.0558 (12)	0.0536 (12)	0.0076 (10)	−0.0010 (10)	−0.0010 (10)
C5	0.0625 (13)	0.0499 (11)	0.0627 (13)	0.0022 (10)	−0.0039 (10)	0.0090 (10)
C3	0.0700 (14)	0.0560 (12)	0.0519 (12)	0.0046 (11)	0.0072 (10)	−0.0024 (10)
C6	0.0678 (14)	0.0590 (12)	0.0456 (11)	−0.0029 (11)	0.0047 (10)	0.0060 (9)
N1	0.0879 (18)	0.0835 (17)	0.0752 (17)	0.0218 (14)	−0.0170 (14)	0.0084 (14)
C8	0.0461 (12)	0.0625 (14)	0.097 (2)	0.0009 (10)	0.0032 (13)	0.0092 (13)
C23	0.0524 (12)	0.0742 (14)	0.0465 (11)	0.0015 (11)	−0.0002 (9)	−0.0048 (10)
C4	0.0650 (14)	0.0589 (13)	0.0673 (14)	0.0125 (11)	0.0070 (11)	0.0006 (11)
C1	0.0585 (13)	0.0636 (13)	0.0587 (13)	−0.0062 (11)	−0.0051 (11)	0.0079 (11)
C22	0.0488 (11)	0.0592 (12)	0.0615 (13)	0.0003 (10)	−0.0001 (10)	−0.0007 (10)
C26	0.0633 (15)	0.0695 (16)	0.096 (2)	0.0115 (12)	−0.0062 (14)	−0.0209 (15)
C25	0.0602 (15)	0.094 (2)	0.0810 (18)	0.0015 (14)	−0.0139 (13)	−0.0276 (15)
C12	0.089 (2)	0.117 (2)	0.0573 (15)	0.0244 (19)	−0.0056 (14)	0.0011 (16)
C13	0.0813 (18)	0.0751 (16)	0.0629 (15)	0.0115 (13)	0.0117 (13)	0.0125 (12)

Geometric parameters (Å, º)

F2—C20	1.350 (2)	C18—F1	1.355 (3)
O6—C16	1.272 (3)	C10—H10	0.9300
N2—C14	1.413 (3)	C21—H21A	0.9700
N2—C10	1.338 (3)	C21—H21B	0.9700
N2—C11	1.459 (3)	C21—C22	1.508 (3)
O5—H5	0.8200	C7—C6	1.382 (3)
O5—C8	1.315 (4)	C7—O1	1.341 (3)
O2—C1	1.277 (3)	C11—H11	0.9800
N5—H5A	0.99 (3)	C11—C12	1.486 (3)
N5—H5B	0.91 (3)	C11—C13	1.479 (4)
N5—C23	1.505 (3)	C5—C6	1.386 (3)
N5—C22	1.496 (3)	C5—N1	1.379 (3)
C20—C14	1.388 (3)	C5—C4	1.392 (3)
C20—C19	1.396 (3)	C3—H3	0.9300
C14—C15	1.432 (3)	C3—C4	1.367 (3)
O3—C1	1.247 (3)	C6—H6	0.9300
O4—C8	1.210 (4)	N1—H1A	0.78 (4)
N4—C24	1.459 (3)	N1—H1B	0.96 (5)
N4—C19	1.382 (3)	C23—H23	0.9800
N4—C21	1.453 (3)	C23—C25	1.512 (4)
C17—N3	1.365 (3)	C4—H4	0.9300
C17—C18	1.386 (3)	C22—H22	0.9800
C17—C15	1.418 (3)	C22—C26	1.519 (3)

C24—H24A	0.9700	C26—H26A	0.9600
C24—H24B	0.9700	C26—H26B	0.9600
C24—C23	1.510 (3)	C26—H26C	0.9600
C16—C9	1.417 (3)	C25—H25A	0.9600
C16—C15	1.447 (3)	C25—H25B	0.9600
N3—H3A	0.8626	C25—H25C	0.9600
N3—H3B	0.91 (3)	C12—H12A	0.9700
C19—C18	1.380 (3)	C12—H12B	0.9700
C2—C7	1.401 (3)	C12—C13	1.483 (5)
C2—C3	1.394 (3)	C13—H13A	0.9700
C2—C1	1.478 (3)	C13—H13B	0.9700
C9—C10	1.364 (4)	O1—H1	1.02 (4)
C9—C8	1.483 (3)		

C14—N2—C11	121.80 (17)	N2—C11—C13	120.7 (2)
C10—N2—C14	119.53 (19)	C12—C11—H11	115.0
C10—N2—C11	118.54 (19)	C13—C11—H11	115.0
C8—O5—H5	109.5	C13—C11—C12	60.0 (2)
H5A—N5—H5B	113 (2)	C6—C5—C4	118.8 (2)
C23—N5—H5A	106.0 (15)	N1—C5—C6	120.9 (3)
C23—N5—H5B	107.1 (17)	N1—C5—C4	120.3 (3)
C22—N5—H5A	108.8 (16)	C2—C3—H3	118.7
C22—N5—H5B	108.4 (17)	C4—C3—C2	122.6 (2)
C22—N5—C23	113.76 (17)	C4—C3—H3	118.7
F2—C20—C14	120.82 (19)	C7—C6—C5	120.9 (2)
F2—C20—C19	116.15 (18)	C7—C6—H6	119.5
C14—C20—C19	122.9 (2)	C5—C6—H6	119.5
N2—C14—C15	118.78 (18)	C5—N1—H1A	112 (3)
C20—C14—N2	122.52 (19)	C5—N1—H1B	116 (2)
C20—C14—C15	118.70 (19)	H1A—N1—H1B	120 (4)
C19—N4—C24	120.98 (19)	O5—C8—C9	115.7 (2)
C19—N4—C21	122.72 (18)	O4—C8—O5	120.6 (2)
C21—N4—C24	112.94 (17)	O4—C8—C9	123.6 (3)
N3—C17—C18	118.1 (2)	N5—C23—C24	108.90 (18)
N3—C17—C15	124.2 (2)	N5—C23—H23	108.8
C18—C17—C15	117.7 (2)	N5—C23—C25	109.0 (2)
N4—C24—H24A	109.5	C24—C23—H23	108.8
N4—C24—H24B	109.5	C24—C23—C25	112.4 (2)
N4—C24—C23	110.9 (2)	C25—C23—H23	108.8
H24A—C24—H24B	108.0	C5—C4—H4	120.0
C23—C24—H24A	109.5	C3—C4—C5	119.9 (2)
C23—C24—H24B	109.5	C3—C4—H4	120.0
O6—C16—C9	120.9 (2)	O2—C1—C2	117.2 (2)
O6—C16—C15	121.8 (2)	O3—C1—O2	122.8 (2)
C9—C16—C15	117.3 (2)	O3—C1—C2	120.0 (2)
C17—N3—H3A	109.2	N5—C22—C21	109.50 (19)
C17—N3—H3B	120.3 (19)	N5—C22—H22	108.8
H3A—N3—H3B	129.4	N5—C22—C26	109.40 (19)

N4—C19—C20	123.7 (2)	C21—C22—H22	108.8
C18—C19—C20	116.44 (19)	C21—C22—C26	111.4 (2)
C18—C19—N4	119.9 (2)	C26—C22—H22	108.8
C7—C2—C1	122.0 (2)	C22—C26—H26A	109.5
C3—C2—C7	117.0 (2)	C22—C26—H26B	109.5
C3—C2—C1	121.0 (2)	C22—C26—H26C	109.5
C16—C9—C8	121.7 (2)	H26A—C26—H26B	109.5
C10—C9—C16	120.0 (2)	H26A—C26—H26C	109.5
C10—C9—C8	118.3 (2)	H26B—C26—H26C	109.5
C19—C18—C17	124.8 (2)	C23—C25—H25A	109.5
F1—C18—C17	116.6 (2)	C23—C25—H25B	109.5
F1—C18—C19	118.6 (2)	C23—C25—H25C	109.5
N2—C10—C9	124.6 (2)	H25A—C25—H25B	109.5
N2—C10—H10	117.7	H25A—C25—H25C	109.5
C9—C10—H10	117.7	H25B—C25—H25C	109.5
N4—C21—H21A	109.7	C11—C12—H12A	117.8
N4—C21—H21B	109.7	C11—C12—H12B	117.8
N4—C21—C22	109.91 (18)	H12A—C12—H12B	114.9
H21A—C21—H21B	108.2	C13—C12—C11	59.76 (18)
C22—C21—H21A	109.7	C13—C12—H12A	117.8
C22—C21—H21B	109.7	C13—C12—H12B	117.8
C14—C15—C16	119.9 (2)	C11—C13—C12	60.24 (19)
C17—C15—C14	119.41 (19)	C11—C13—H13A	117.7
C17—C15—C16	120.7 (2)	C11—C13—H13B	117.7
C6—C7—C2	120.8 (2)	C12—C13—H13A	117.7
O1—C7—C2	121.1 (2)	C12—C13—H13B	117.7
O1—C7—C6	118.1 (2)	H13A—C13—H13B	114.9
N2—C11—H11	115.0	C7—O1—H1	104 (2)
N2—C11—C12	120.0 (2)		

F2—C20—C14—N2	−3.8 (3)	C2—C3—C4—C5	0.1 (4)
F2—C20—C14—C15	175.22 (19)	C9—C16—C15—C14	−0.1 (3)
F2—C20—C19—N4	3.7 (3)	C9—C16—C15—C17	−179.30 (19)
F2—C20—C19—C18	−176.5 (2)	C18—C17—C15—C14	0.6 (3)
O6—C16—C9—C10	179.3 (2)	C18—C17—C15—C16	179.9 (2)
O6—C16—C9—C8	−0.6 (3)	C10—N2—C14—C20	179.1 (2)
O6—C16—C15—C14	179.55 (19)	C10—N2—C14—C15	0.1 (3)
O6—C16—C15—C17	0.3 (3)	C10—N2—C11—C12	−32.2 (3)
N2—C14—C15—C17	179.81 (18)	C10—N2—C11—C13	−103.1 (3)
N2—C14—C15—C16	0.6 (3)	C10—C9—C8—O5	179.2 (2)
N2—C11—C12—C13	−110.3 (3)	C10—C9—C8—O4	−0.4 (4)
N2—C11—C13—C12	109.2 (3)	C21—N4—C24—C23	59.4 (3)
C20—C14—C15—C17	0.8 (3)	C21—N4—C19—C20	31.9 (4)
C20—C14—C15—C16	−178.49 (19)	C21—N4—C19—C18	−147.9 (2)
C20—C19—C18—C17	1.7 (4)	C15—C17—C18—C19	−1.9 (4)
C20—C19—C18—F1	−176.96 (19)	C15—C17—C18—F1	176.70 (18)
C14—N2—C10—C9	−1.4 (3)	C15—C16—C9—C10	−1.1 (3)
C14—N2—C11—C12	151.9 (2)	C15—C16—C9—C8	179.0 (2)

C14—N2—C11—C13	81.1 (3)	C7—C2—C3—C4	−1.4 (3)
C14—C20—C19—N4	−179.9 (2)	C7—C2—C1—O2	−2.5 (3)
C14—C20—C19—C18	−0.1 (3)	C7—C2—C1—O3	176.9 (2)
N4—C24—C23—N5	−53.8 (3)	C11—N2—C14—C20	−5.1 (3)
N4—C24—C23—C25	−174.7 (2)	C11—N2—C14—C15	175.90 (19)
N4—C19—C18—C17	−178.5 (2)	C11—N2—C10—C9	−177.3 (2)
N4—C19—C18—F1	2.9 (3)	C3—C2—C7—C6	2.2 (3)
N4—C21—C22—N5	55.5 (2)	C3—C2—C7—O1	−177.9 (2)
N4—C21—C22—C26	176.7 (2)	C3—C2—C1—O2	179.3 (2)
C24—N4—C19—C20	−125.9 (2)	C3—C2—C1—O3	−1.3 (4)
C24—N4—C19—C18	54.3 (3)	C6—C5—C4—C3	0.4 (4)
C24—N4—C21—C22	−59.7 (3)	N1—C5—C6—C7	178.4 (2)
C16—C9—C10—N2	1.9 (3)	N1—C5—C4—C3	−177.6 (2)
C16—C9—C8—O5	−0.9 (3)	C8—C9—C10—N2	−178.2 (2)
C16—C9—C8—O4	179.5 (2)	C23—N5—C22—C21	−54.5 (3)
N3—C17—C18—C19	177.6 (2)	C23—N5—C22—C26	−176.8 (2)
N3—C17—C18—F1	−3.8 (3)	C4—C5—C6—C7	0.4 (3)
N3—C17—C15—C14	−178.8 (2)	C1—C2—C7—C6	−176.1 (2)
N3—C17—C15—C16	0.4 (4)	C1—C2—C7—O1	3.8 (3)
C19—C20—C14—N2	179.92 (19)	C1—C2—C3—C4	176.9 (2)
C19—C20—C14—C15	−1.1 (3)	C22—N5—C23—C24	53.3 (3)
C19—N4—C24—C23	−140.8 (2)	C22—N5—C23—C25	176.3 (2)
C19—N4—C21—C22	140.8 (2)	O1—C7—C6—C5	178.3 (2)
C2—C7—C6—C5	−1.7 (3)		

Hydrogen-bond geometry (Å, º)

*Cg*6 is the centroid of the C2–C7 ring.

D—H···*A*	*D*—H	H···*A*	*D*···*A*	*D*—H···*A*
O1—H1···O2	1.02 (4)	1.60 (4)	2.529 (3)	149 (3)
N3—H3*A*···O6	0.86	1.92	2.648 (3)	142
N3—H3*A*···O1^{i}	0.86	2.52	2.965 (3)	113
N3—H3*B*···F1	0.91 (3)	2.29 (3)	2.637 (3)	102 (2)
O5—H5···O6	0.82	1.73	2.497 (3)	154
N5—H5*A*···O2^{ii}	0.99 (3)	1.74 (3)	2.715 (3)	167 (2)
N5—H5*B*···O3	0.91 (3)	1.85 (3)	2.754 (3)	172 (3)
N1—H1*B*···*Cg*6^{iii}	0.95 (4)	2.46 (5)	3.326 (3)	153 (4)

Symmetry codes: (i) *x*+1/2, −*y*−1/2, *z*−1/2; (ii) −*x*, −*y*, −*z*+1; (iii) −*x*+1/2, *y*−1/2, −*z*+3/2.